Title:

Environmental contaminants modulate transport activity of zebrafish (*Danio rerio*) multidrug and toxin extrusion protein 3 (Mate3/Slc47a2.1)

Authors: Lana Vujica[1], Jovica Lončar[1], Lana Mišić[1,5], Bono Lučić[2], Katarina Radman[3], Ivan Mihaljević[1], Branimir Bertoša[3], Josip Mesarić[4], Marina Horvat[1,6], Tvrtko Smital[1,*]

[1]Laboratory for Molecular Ecotoxicology, Division for Marine and Environmental Research, Ruđer Bošković Institute, Bijenička cesta 54, 10 000 Zagreb, Croatia

[2]NMR Center, Ruđer Bošković Institute, Bijenička cesta 54, 10 000 Zagreb, Croatia

[3]Department of Chemistry, Faculty of Science, University of Zagreb, Horvatovac 102a, 10 000 Zagreb, Croatia

[4]Centre for Informatics and Computing, Ruđer Bošković Institute, Bijenička cesta 54, 10 000 Zagreb, Croatia

[5]Present address: Gredice 18, Puhovo, 10370 Dugo Selo, Croatia

[6]Present address: Centre for Medical Genetics Ghent, Ghent University Hospital, Department of Biomolecular Medicine, Ghent University, 9000 Ghent, Belgium

*corresponding author: smital@irb.hr; Laboratory for Molecular Ecotoxicology, Division for Marine and Environmental Research, Ruđer Bošković Institute, Bijenička cesta 54, 10 000 Zagreb, Croatia; Tel. +385 1 456 108

Abstract

Zebrafish Mate3 is one of six co-orthologs of human multidrug and toxin extrusion proteins. It is highly expressed in the kidneys, intestine, testes, and brain of males. Initial interaction studies showed its interaction with xenobiotic compounds, suggesting a role in the efflux of toxic compounds. In this study, we aimed to test various environmental pollutants for their interaction with zebrafish Mate3. We developed a stable zebrafish Mate3 cell line (FlpIn/drM3) and optimized a high-throughput screening assay using DAPI and ASP^+ as fluorescent model substrates. To gain insight into the structure and function of the Mate3 protein and relate these to the results of the DAPI and ASP^+ transport measurements, we predicted its 3D structure using the AlphaFold2

algorithm. A 3D structure with high per residue confidence scores with 13 transmembrane segments (TMs) was obtained, with topology and mutual positioning characteristic of the Mate3 protein family in a shape open to the extracellular part. Molecular docking methods were used to identify DAPI and ASP^+ binding sites on the surface and in the center of the protein cavity. Because our kinetics experiments combined with molecular docking indicated that there may be additional active sites in zebrafish Mate3, additional cytotoxicity experiments were performed and highly potent Mate3 interactors (substrates and inhibitors) were identified from a set of 55 different environmentally relevant compounds. Our results suggest that some of the identified interactors may be of environmental concern, as their interaction with Mate3 could lead to an impairment of its normal efflux function, making fish more sensitive to harmful substances commonly released into the aquatic environment. Finally, the quality of zebrafish Mate3 structures predicted by the AlphaFold2 algorithm opens up the possibility of successfully using this tool for *in silico* research on transport preferences of other Mate proteins.

Keywords: (3-6max) zebrafish, Mate3, *in vitro* interaction studies, AlphaFold2 3D structure, molecular docking

1. Introduction

The cell membrane serves as a selective barrier and is one of the crucial determinants of absorption, distribution, metabolism and excretion (ADME) of xenobiotic and physiological compounds. Apart from transport, lipid membranes are essential for maintaining the structure and functions of transport proteins (Xie, 2008). Membrane transport proteins belonging to two superfamilies – the ATP-binding cassette (ABC) and the solute carrier family (SLC) – are considered crucial for the uptake and elimination processes (Shin et al., 2015). Among the numerous proteins present in the cell membrane, uptake transport proteins represent the initial phase of cellular detoxification (phase 0). After compounds enter the cell, they are further metabolized by phase I and II detoxification enzymes and finally eliminated from the cell by efflux transporters. ABC transporters are a large superfamily of ATP-dependent proteins that mediate the active transport of structurally and chemically diverse physiological substrates across cell membranes. In contrast

to MATEs (Multidrug and Toxin Extrusion Proteins), the role of ABC transporters in multidrug (MDR) and multixenobiotic resistance (MXR) phenotypes in mammals and fish has been extensively studied (Luckenbach et al., 2014). MATE/Mate proteins (MATEs in humans, Mates in other species; gene name *SLC47* in humans, *slc47* in other species) belong to the superfamily of solute carriers (SLCs). They function as bidirectional transporters (efflux of substrates involves proton-coupled electroneutral exchange) and primarily mediate elimination of cationic compounds, but can also transport anionic and zwitterionic compounds (Damme et al., 2011). MATEs/Mates are 400-600 amino acids long and consist of 12-13 transmembrane domains (TMDs) with an intracellular N terminus and an intracellular or extracellular C terminus (Zhang et al., 2012; Zhang & Wright, 2009). In humans, two MATE proteins have been identified, hMATE1 and hMATE2, with two splice variants hMATE2-K and hMATE2-B (Masuda et al., 2006). Two MATE proteins are also found in mice (MATE1a and MATE2: Hiasa et al., 2006, 2007; Kobara et al., 2008), rats (Mate1 and Mate2: Ohta et al., 2006; Hiasa et al., 2007), and rabbits (Mate1 and Mate2-K; Zhang et al., 2007).

We have previously shown that there are six *mate* genes in the zebrafish (*Danio rerio*) genome arranged in two clusters, namely *mate3*, *4*, and *6* on chromosome 21 and *mate5*, *7*, and *8* on chromosome 15, which arose from a genome duplication event (Lončar et al., 2016). We also analyzed the expression of *mate* genes in zebrafish embryos and adults and found that all *mate* transcripts are constitutively and differentially expressed during embryonic development, suggesting that they probably play specific roles during early development. In addition, all six zebrafish mates are ubiquitously expressed in the analyzed tissues of adult zebrafish, with the highest expression in the kidneys and testes and to a lesser extent in the liver and brain. Finally, our results indicated a low affinity of zebrafish Mate3 for physiological compounds.

Therefore, to gain better insight into the potential role of the zebrafish Mate3 transporter in cellular defense, in this study we tested a range of 55 environmentally relevant xenobiotics, including industrial chemicals, pesticides, and pharmaceuticals, for their interaction with zebrafish Mate3. However, to study the relationship between structure and function of a membrane transport protein, reliable insight into its three dimensional (3D) structure is required, which can either be determined experimentally or predicted by *in silico* models (Clerbaux et al., 2018). Since it is much more difficult to determine the structure of membrane than that of soluble proteins, the number of

experimentally determined 3D structures of membrane proteins is about ten times smaller than that of soluble proteins (Dobson et al., 2023). Moreover, it is known that there is a large difference between soluble and membrane proteins in the composition of the medium in which they reside, obtain their 3D structure, and in which soluble and membrane proteins function. Consequently, it would be of great advantage if the available algorithms could predict the structure of a membrane protein reasonably well. One such algorithm that has recently made extraordinary and unprecedented progress is AlphaFold (Jumper et al., 2021), and in this study we used the 3D structure of the zebrafish Mate3 predicted by AlphaFold as an additional *in silico* tool to verify our experimental data. The correctness of the predicted 3D structure was further tested by comparisons with other bioinformatics tools and algorithms for predicting the position of transmembrane segments and the topology of membrane proteins (Bernsel et al., 2009), as well as with experimentally determined 3D structures of other membrane proteins from the same family and with other structural and functional data and findings from the literature.

The findings from the 3D structure of zebrafish Mate3 and the associated molecular docking analysis of the interaction of Mate3 with the model substrates DAPI (4',6-diamidino-2-phenylindole) and ASP^+ (4-(4 (dimethylamino)styryl)-N-methylpyridinium iodide) were then used as additional indicators, relevant for determination of the nature of the interaction with the tested xenobiotics using the developed HEK293 Flp in-cell line stably overexpressing Mate3. The compounds that showed significant interaction potency, defined as inhibition of DAPI uptake, were further characterized. Because both our initial kinetic experiments and molecular docking studies indicated that there may be additional active sites in zebrafish Mate3, additional cytotoxicity experiments were performed and highly potent Mate3 interactors (substrates and inhibitors) were identified. In addition, the interaction specificities of selected compounds with the zebrafish Mate3 transporter are presented and compared with the mammalian Mates and the zebrafish Oct1 cationic transporter.

2. Materials and methods

2.1 Chemicals

All tested compounds, model fluorescent substrates and interactors alike, were purchased from Sigma-Aldrich (Taufkirchen, Germany) or Alfa Aesar (Ward Hill, MA, USA) unless stated otherwise. An overview of basic characteristics of tested compounds is shown in Supplementary Material (Table S8).

2.2 Development of the Mate3-expressing cell line

The full-length zebrafish *mate3* sequence (gene bank: NM_001080179.1) was amplified from zebrafish cDNA originating from male kidneys using high-fidelity Phusion DNA polymerase (Finnzymes, Vantaa, Finland) in the polymerase chain reaction. Primers were specifically designed with NheI and EcoRI restriction sites in the forward primer and NotI and KpnI restriction sites in the reverse primer. The resulting amplicon was cloned into the pcDNA3.1/His vector (Thermo Fisher Scientific, Waltham, USA), which was linearized with a combination of the restriction enzymes NheI and NotI.

Further steps were performed as described in detail in Lončar and Smital, 2018. The developed cell lines were designated FlpIn/Mock and FlpIn/drM3, the first stably transfected with an empty plasmid and the second stably transfected with a plasmid carrying the zebrafish Mate3 (drM3) protein coding sequence.

The expression levels of the human *SLC47A1* and *SLC47A2* genes and the zebrafish *mate3* genes in the cells were quantified by qPCR and expressed as mean normalized expression (MNE), which is the relative expression level of the gene of interest compared to the expression level of the housekeeping gene (*EEF1A1*).

2.3 Activity of the Mate3 transport protein

Cellular uptake experiments were performed using FlpIn/Mock and FlpIn/drM3 cells in 96-well plates as previously described (Lončar and Smital, 2018), with minor modifications. The final concentration of cells was 7.5 x 10^4 which was sufficient to reach confluence 24 or 48 h after cultivation. Mate3 transport protein activity was assessed using the fluorescent substrates DAPI and ASP^+, which can be measured in real-time due to an increase in fluorescent signal after intercalation into DNA. Real-time uptake kinetics were monitored for 5-10 min by measuring fluorescence signals at the following excitation and emission wavelengths: 360/460 nm for DAPI, and 450/590 nm for ASP^+. To obtain transporter-specific uptake, uptake in mock-transfected cells

was subtracted. Calibration curves of fluorescent dyes in 0.1% SDS and cell matrix dissolved in 0.1% SDS were determined (except for ASP^+, where cell matrix was used without detergent), and transport rates of fluorescent substrates were calculated and expressed as pmol substrate per mg protein per minute. The resulting linear calibration curves were identical in SDS, where applied, and in the dissolved cell matrix. Total cell protein concentration was measured using the Bradford assay (Bradford, 1976).

After determining the transport kinetics for fluorescent dyes, DAPI was selected for further inhibition assays. DAPI is a fluorescent dye commonly used for staining cell nuclei and emits blue fluorescent light after excitation with ultraviolet light only when intercalated into DNA double strands (Kapuscinski, 1995). Therefore, using the DAPI-based transport activity assay, we selected and tested a number of known xenobiotic interactors of mammalian MATEs/Mates. The identification of Mate3 interactors was based on functional transport activity assays previously developed in our group (described in detail in Lončar & Smital, 2018). The selection of xenobiotic compounds was further refined based on their positive charge at physiological pH and/or their presence in the environment. The transport activity assays were performed in the same transport medium as the substrate uptake experiments and the DAPI concentration used was 3 μM. Compounds tested for interaction were initially tested at a concentration of 50 μM unless stated otherwise. If the interacting compound showed an inhibition of DAPI uptake greater than 25% (arbitrary threshold), its concentration-response curves were determined and the corresponding IC_{50} values were calculated. Compounds with an IC_{50} of <1 μM were designated as very strong (VSt) interactors, and an IC_{50} of 1–29 μM indicated strong (St), an IC_{50} of 30–99 μM indicated moderate (M), an IC_{50} of 100–999 μM weak (W) interaction strength, and interactors with an IC_{50} above 1000 μM were considered very weak (VW) interactors.

The number of Mate3 binding sites was probed by measuring the shift in K_m and V_{max} values for one transported model substrate (DAPI or ASP^+) in the presence of the other model substrate as interactor (DAPI, ASP^+, or berberine) at a concentration equal to the IC_{50} value with varying concentrations of the transported substrate. All experiments were repeated at least three times in duplicate determinations. Uptake in mock cells was subtracted to obtain transporter-specific uptake. An increase in K_m at constant transport rate in the presence of an interactor indicates competitive inhibition, and the compound is designated as a substrate. A different pattern is present

when no change in K_m occurs and V_{max} decreases, indicating noncompetitive inhibition. Additional details on data analysis can be found in Supplementary Material **(**chapter 1.2 Data analysis / Calculation).

2.4 Prediction of Mate3 (and Mate 7) protein structures by AlphaFold algorithm

AlphaFold2 (Jumper et al., 2021) is installed as a Singularity container on the BURA HPC cluster at the University of Rijeka, Croatia. AlphaFold predictions ran on a single node with two Xeon E5-2690 v3 processors (24 physical cores per node), 64 GB memory, and a Lustre filesystem used for the AlphaFold database. The official Docker image (Jumper et al., 2021) was used for the installation, and converted to a Singularity container to be supported on BURA HPC. Prediction was performed using a full database version of AlphaFold2, creating five monomer models from which the most accurate was selected. The accuracy of the predicted 3D protein structure was determined by the AlphaFold internal confidence scoring system pLDDT, which corresponds to the predicted score of the model on the lDDT-Cα metric (Mariani et al., 2013). In this case, if parts of the 3D structure at the N- or C-end are of lower reliability, they are removed to prevent a possible reversal of the orientation of the protein with respect to the membrane.

Positioning the 3D structure of a membrane protein in the membrane (lipid bilayer) involves calculating the interactions and free energies of the protein in the membrane and predicting the membrane deformations caused by the protein, taking into account the hydrophobic thicknesses of the artificial lipid bilayers (Lomize et al., 2011). The whole procedure was optimised on a representative set of membrane proteins from the OPM database (Lomize et al., 2012), whose 3D structure was determined. We used the PPM 3.0 method implemented on the web server (https://opm.phar.umich.edu/ppm_server3). Additional details on protein topology prediction, prediction accuracy, and homology analyses of the zebrafish Mate3 protein can be found in the Supplementary Material (chapter 1.1 Protein structure prediction).

2.5 Molecular docking

The docking study was performed using the predicted 3D structure of the Mate3 protein (Slc47a2.1; U3MYZ9_DANRE). As an additional control, we also extracted an example of the

Mate7 protein predicted using the AlphaFold algorithm (Jumper et al., 2021) based on amino acid sequence. Only protein atoms were used for the docking calculations. Hydrogen atoms were added using the MolProbity program (Williams et al., 2018). Two putative model substrates for zebrafish Mate3 were used for the docking study: ASP^+ and DAPI. Their 3D structures were built *in silico* using the Maestro program (Schrödinger, 2021). Docking preparation was performed with AutoDock Tools 4 (Morris et al., 2009) using default settings. Four sets of docking calculations were performed for each protein and compound. In the first set of docking calculations, the grid size was set to the maximum (126 Å x 126 Å x 126 Å) and the entire protein was included ("blind docking") (Fig. S12A). The other docking calculations were performed with a smaller grid (22 Å x 22 Å x 22 Å) shifted across the entire transport cavity such that each docking set covers one part of the transportation cavity (Fig. S12B and Table S6). Docking studies were performed using AutoDock Vina 1.1.2 (Trott & Olson, 2009) with search exhaustiveness set to 32. Results were analyzed using AutoDock Vina, Maestro and VMD (Humphrey et al., 1996).

2.6 Cytotoxicity assays / Cell viability assay

The MTT (3-(4,5-dimethylthiazol-2-yl)-2,5-diphenyltetrazolium bromide) colorimetric tetrazolium reduction assay (Mosmann, 1983) was used to determine cytotoxicity as described in detail in (Lončar & Smital, 2018). Briefly, exposure lasted 72 h and formazan production was measured at 578 nm, using 750 nm as the reference wavelength. Cytotoxicity was expressed as a percentage of the product formed relative to the corresponding control value (untreated cells) and the results were used for *in vitro* verification of the type of the interaction and the possible (eco)toxicological role of zebrafish Mate3.

3. Results

3.1 Gene expression analysis

Mate3 expression was quantified in transfected and mock cells and compared to human MATEs expression (Fig. S1). The results obtained confirmed a notable difference in the transcription level of the *mate3* gene compared to the human *SLC47A1* and *SLC47A2* genes, indicating successful transfection. Accordingly, the transcript level of the *mate3* gene in the FlpIn/drM3 cell line, expressed as mean normalized value (MNE) was $296{,}277 \times 10^6$, whereas the transcript level of the

SLC47A1 gene encoding the human MATE1 transport protein was 50-fold lower (5,859 × 10^6), and the transcript level of the *SLC47A2* gene encoding human MATE2-K was negligible (9 × 10^6).

3.2 Kinetic parameters of Mate3 fluorescent substrates

The basic kinetic parameters were determined for two fluorescent substrates and the corresponding values are listed in Table 1. The values obtained for DAPI and ASP^+ agreed well with the results obtained using the transient assay system (Lončar et al., 2016). Based on the results of the kinetic experiments (Figs. S2 and S3), and the ability to measure uptake in real-time and at physiologically relevant pH 7.4, DAPI was selected as the model fluorescent zebrafish Mate3 substrate for further high-throughput experiments.

Table 1. Zebrafish Mate3 mediated uptake of the fluorescent dyes DAPI and ASP^+ as evaluated by determining the kinetic parameters K_m (μM) and V_{max} (pmol/mg protein/min). Mean values for each parameter were obtained from at least three independent experiments, with 95% confidence intervals (CI) provided. Corresponding dose-response curves are depicted in Figs. S2 and S3.

	K_m (μM)	95% CI	V_{max} (pmol/min/mg)	95% CI	N
DAPI	2.19	1.47 - 2.91	409	358 - 460	6
ASP^+	5.51	3.79 - 7.23	83.2	71.2 - 95.2	3

3.3 Probing the zebrafish Mate3 substrate binding site

Kinetic experiments measuring DAPI dose-response in the presence of ASP^+ provided a strong indication of non-competitive inhibition (Table 2; Fig. S5C). A similar result was obtained when ASP^+ dose-response was measured in the presence of DAPI (Table S1; Fig. S4B). These results indicate that DAPI and ASP^+ bind to different Mate3 regions, suggesting that zebrafish Mate3 has multiple binding sites and that Michaelis-Menten kinetic experiments cannot be used to reliably distinguish the type of the interaction. Therefore, the modulation of toxicity experiments were used instead (Table S2; Fig. S6.).

Table 2. Determination of the type of interaction of the model substrate DAPI with zebrafish Mate3. Fluorescent dyes ASP^+ and berberine were used as model interactors, and the kinetic parameters of DAPI uptake, including apparent K_m ($K_{m,app}$) and apparent V_m ($V_{m,app}$), were determined with 95% confidence intervals (CI), based on a representative example of at least three independent experiments, each performed in duplicate. To calculate the IC_{50}, data from at least three independent experiments were analyzed using the sigmoidal four-parameter dose-response model (variable slope) in GraphPad Prism 8.

	IC_{50} [µM], n=3	95% CI	$K_{m,app}$	95% CI	$V_{m,app}$	95% CI	TOI
DAPI	NA	NA	4.50	3.32 - 5.69	401	345 - 457	NA
ASP^+	13.4	11.3 - 15.7	4.45	3.39 - 5.52	252	224 - 281	I
Berberine	4.91	3.70 - 6.53	13.3	9.45 - 17.2	498	403 - 594	S

NA – not applicable

3.4 Protein structure prediction

The above mentioned experimental results were further supported by homology modelling and molecular docking calculations. The 3D structures of Mate3 and Mate7 (for comparison purposes) were predicted using the AlphaFold2 algorithm and positioned in the membrane as described in Methods (Fig. S7A and B). Their PDB structures can be found in the Supplementary Material (Mate3.pdb and Mate7.pdb files). Using the PPM 3.0 method, 13 TM segments were identified in both structures and their positions in the sequences were indicated (Table S3A and B). The positions of the TM segments were consistent with those predicted by the TOPCONS method (Bernsel et al., 2009) (Table S4) and with the 2D topology of the protein (Figure S8). The topology and the location of TM segments predicted by the TOPCONS consensus method were reliable (Fig. S9) and agreed with the predictions obtained starting from the 3D structure of the protein predicted by the AlphaFold2 algorithm and using the PPM 3.0 method/server. The existence of the 13th TM segment is predicted from the 3D structures of Mate3 and Mate7 proteins obtained by the AlphaFold2 algorithm and using the TOPCONS method. The N-terminus of Mate3 and Mate7 proteins is predicted to be in cellular (cytoplasmic) space. Finally, the 3D topology and mutual

positions of the TM segments (helices) are further confirmed by the ΔGassoc (free association energies) of the TM segments (Table S5A) and the most likely association pathway (Table S5B) determined using the TMPfold server (Lomize et al., 2020). The global sequence similarity of Mate3 and Mate7 proteins is 44.7%, and we have additionally labelled the conserved amino acid residues that are functionally important according to literature data (Fig. S11A).

3.5 Molecular docking analysis

Based on the 3D structure positioned in the cell membrane, molecular docking analysis of model Mate substrates DAPI and ASP^+ was performed. The molecular docking studies showed that DAPI has a higher affinity (described by a lower binding energy) for zebrafish Mate3 than ASP^+ (Table S7), which is consistent with the results of the *in vitro* experiments (lower K_m for DAPI; Table 1). The binding affinity of both ligands is energetically more favourable in the middle membrane region of the transport cavity.

The binding of both ASP^+ and DAPI within the transport cavity is stabilized mainly by π–π stacking interactions. The binding of DAPI conformers is additionally stabilized by hydrogen bonds (Figs. 1 and 2), which explains the better binding affinity scores compared to the binding of ASP^+ (Table S7). ASP^+ does not have a hydrogen atom covalently bonded to an electronegative atom, such as nitrogen in DAPI, and is therefore unable to form hydrogen bonds. Furthermore, the best binding modes of DAPI in the outer membrane part of the cavity form hydrogen bonds with residues Gly298, Glu296, and Thr78 (Fig. 1). Some of the lower scoring binding modes of DAPI form π–π stacking interactions with Phe300. Most of the binding modes of ASP^+ form π–π stacking interactions with Phe300 and are sterically stabilized by the surrounding amino acids (Fig. 1). In the middle part of the transport cavity, DAPI and ASP^+ form π–π stacking interactions with Trp292 (Fig. 2). Compared to the best binding modes of ASP^+, the DAPI binding modes form more than two π–π stacking interactions with Trp292 and hydrogen bonds with residues Asn100 and Glu291 (Fig. 2).

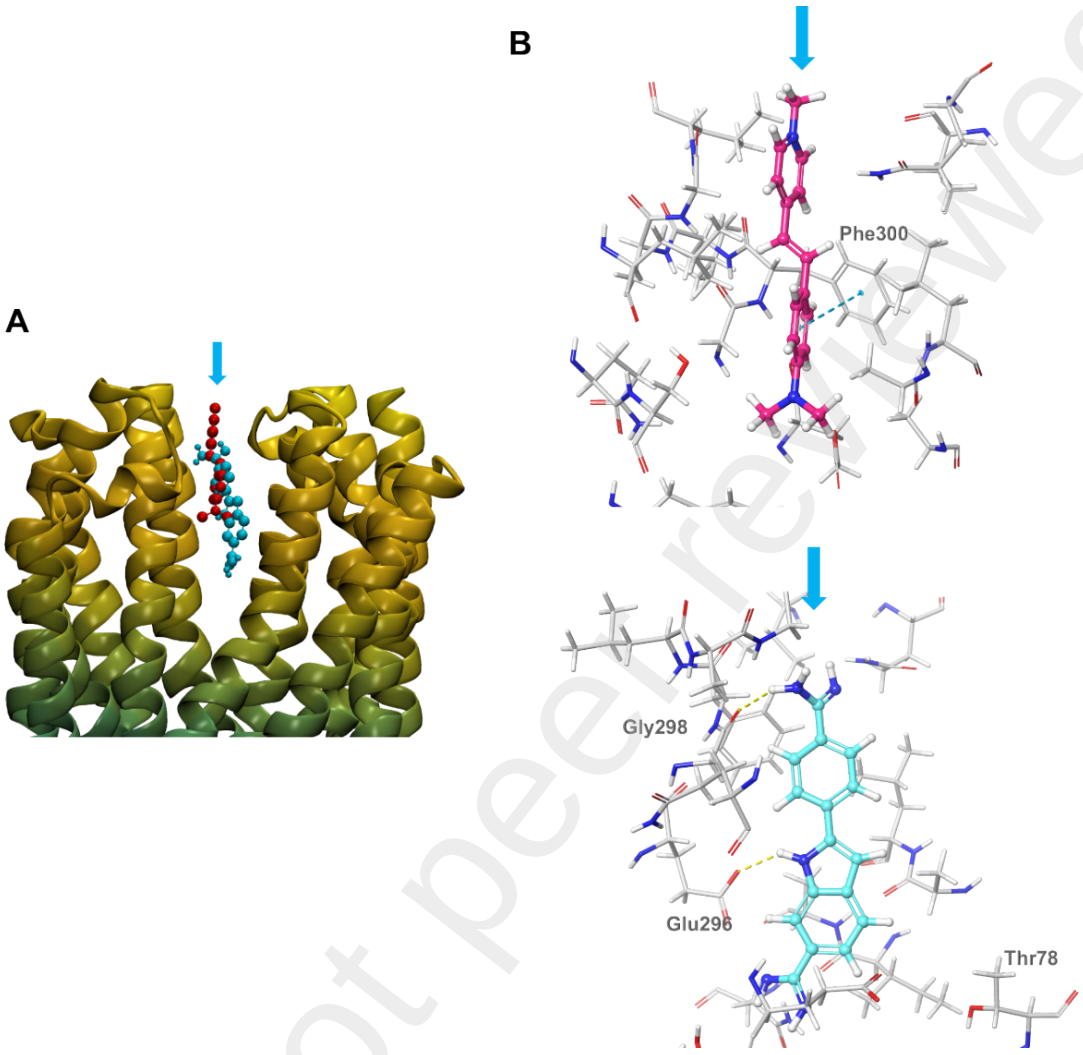

Figure 1. Ligand-Mate3 interactions in the outer membrane part of the transportation cavity. (A) The best binding modes of ASP^+ (red) and DAPI (purple). (B) Interactions of ASP^+ (pink) and DAPI (light blue) with zebrafish Mate3. Hydrogen bonds are shown as yellow and π–π stacking interactions as blue dashed lines.

Compared to the docking calculations performed in the outer membrane part of the zebrafish Mate3 protein, the docking calculations for the zebrafish Mate7 protein showed that the best binding modes of both DAPI and ASP+ form π–π stacking interactions form with His298 and Phe284 and are sterically stabilized by the surrounding amino acids (Fig. S13). The amino acid His298 is structurally specific to Mate7 and has no Mate3 homologue, whereas Phe284 of Mate7 is homologous to Phe300 of Mate3.

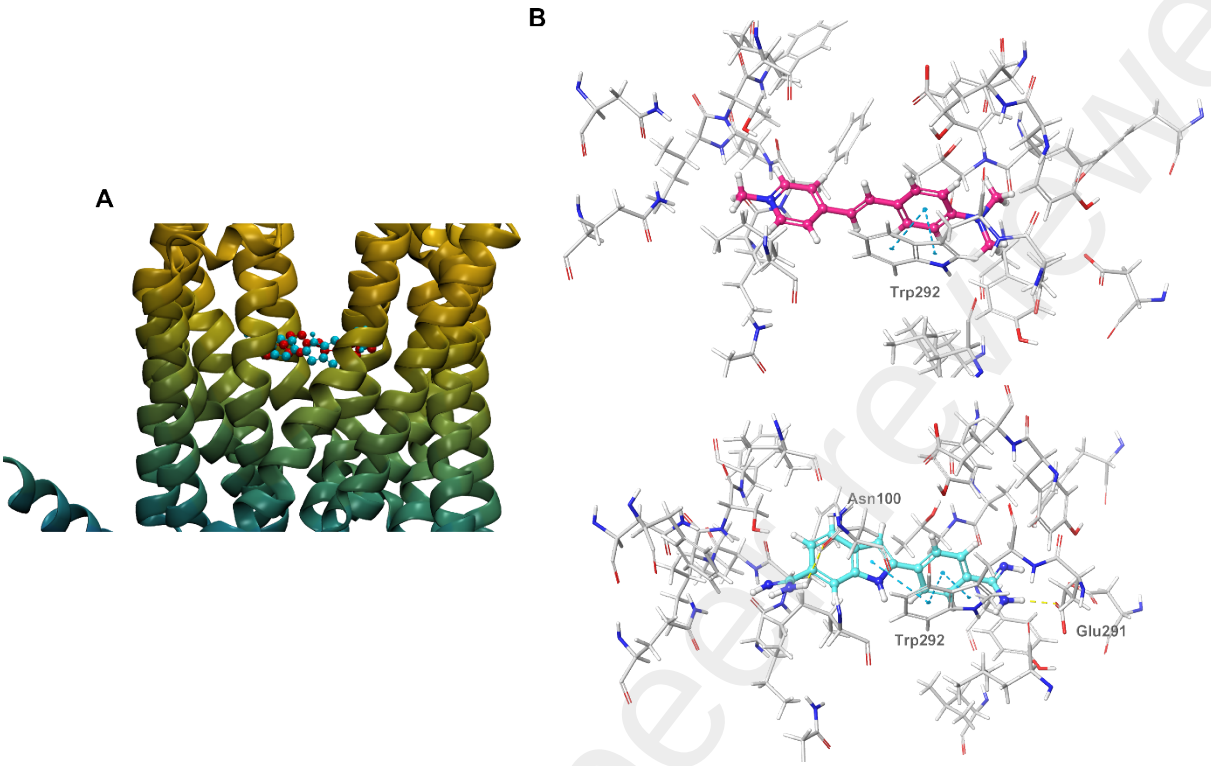

Figure 2. Ligand-Mate3 interactions in the middle membrane region of the transportation cavity. (A) The best binding modes of ASP^+ (red) and DAPI (purple). (B) Interactions of ASP+ (pink) and DAPI (light blue) with zebrafish Mate3. Hydrogen bonds are shown as yellow and π–π stacking interactions as blue dashed lines.

3.6 Interaction of xenobiotic compounds with zebrafish Mate3

The compounds initially tested in our study for their interaction with zebrafish Mate3 were selected based on their occurrence in the environment, their previously reported interaction with mammalian Mates, their positive charge under physiological conditions and their biomedical relevance.

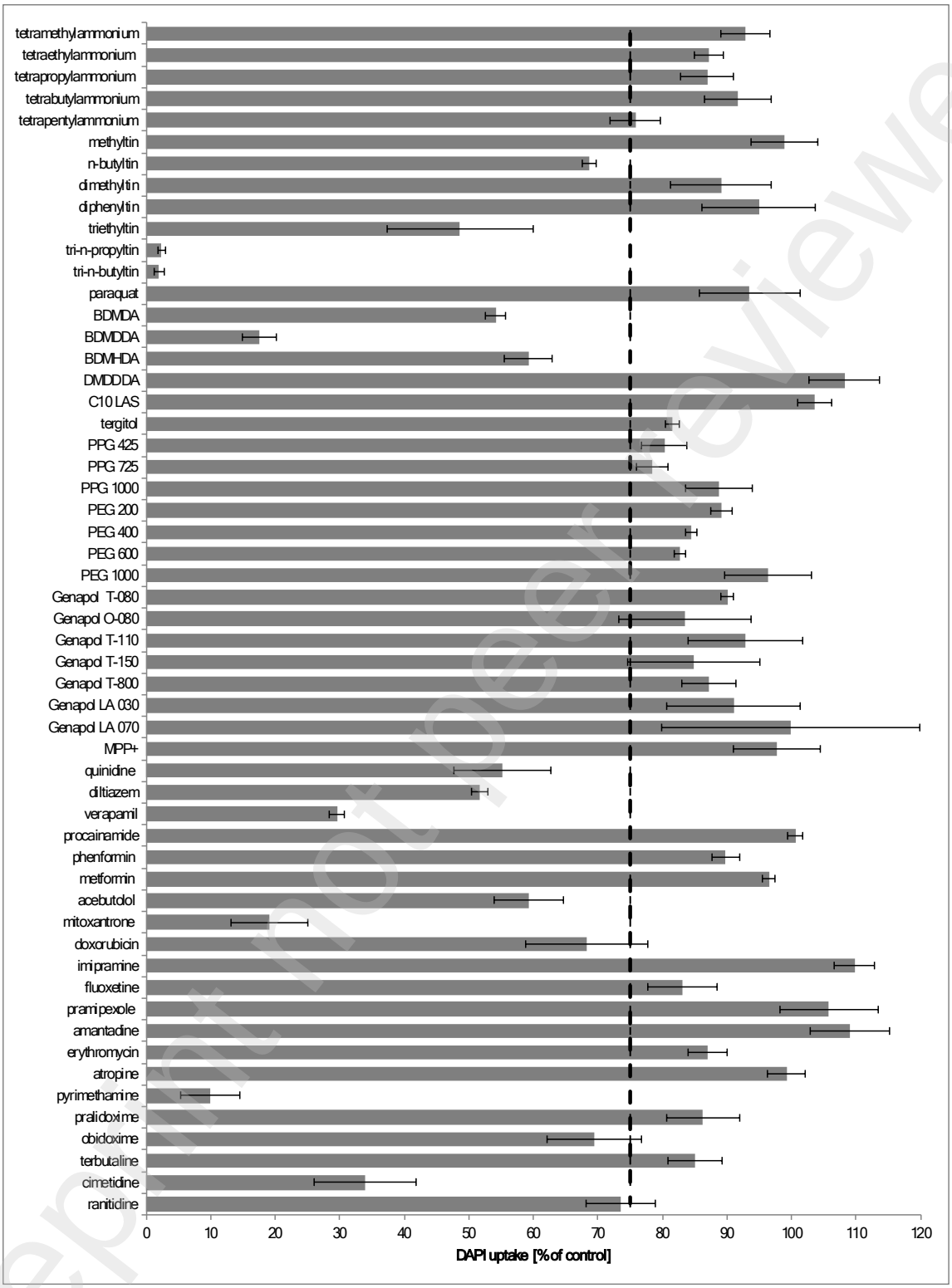

334

335 **Figure 3. Interaction of zebrafish Mate3 with selected compounds was assessed by measuring**
336 **the percentage (%) of DAPI uptake in Flp-In/drM3 cells after 10 minutes of co-incubation**

with each modulator. The concentration of each modulator used was 50 μM, except for mitoxantrone and doxorubicin, which were set to 10 μM. The results were normalized to DAPI uptake in the absence of a modulator, which was set to 100%. Experiments were performed at pH 7.4, and the accumulation of DAPI in mock-transfected cells was subtracted to obtain transporter-specific uptake. The inhibition threshold was arbitrarily set at 25%, represented by the dashed line. Data represent the mean ± standard error (SE) of three independent experiments.

Abbreviations used: TMA – tetramethylammonium, TEA – tetraethylammonium, TPrA – tetrapropylammonium, TBA – tetrabutylammonium, TPenA – tetrapentylammonium, MET – methyltin, nBT - n-butyltin, DMT – dimethyltin, DPheT – diphenyltin, TET – triethyltin, TPrT - tri-n-propyltin, TBT - tri-n-butyltin, PQT – paraquat, BDMDA – benzyldimethyldecylammonium chloride, benzyldimethyldodecylammonium chloride – BDMDDA, benzyldimethylhexadecylammonium chloride – BDMHDA, dimethyldidodecylammonium bromide – DMDDDA, NP9 – tergitol, 1-methyl-4-phenylpyridinum iodide – MPP^+, QUI – quinidine, DILTI – diltiazem, VER – verapamil, PROC – procainamide, PHEN – phenformin, MET – metformin, ACE – acebutolol, MITX – mitoxantrone, DOXO – doxorubicin, IMI – imipramine, FLX – fluoxetine, PRAM – pramipexole, ADA – amantadine, ERT – erythromycin, ATRP – atropine, PYR – pyrimethamine, 2-PAM – pralidoxime, OBI – obidoxime, TER – terbutaline, CIM – cimetidine, RTD – ranitidine.

Of the 55 compounds studied (Table S8), 17 showed inhibition of DAPI uptake above the arbitrary threshold of 25 % (Fig. 3), and their IC_{50} values were further analyzed (Table 3; Fig. S14) to determine the type of the interaction. The compounds that were excluded from further measurements because of their precipitation, deleterious effect on the cell membrane, interference with the fluorescence signal, or a combination of the above factors are listed in Table S11. Because the type of the interaction could not be reliably determined by Michaelis-Menten kinetics due to the possibility of multiple active sites, cytotoxicity experiments were performed instead (the obtained EC_{50} values are listed in Table 4, and the corresponding graphs are shown in Figs. 4 and S15).

3.6.1 Industrial chemicals

Notable interactions with zebrafish Mate3 protein were observed for organotin compounds. Among these, TBT and TPrT showed strong interaction, while moderate interaction was observed for nBT and TET. TBT and TPrT were found to be strong non-competitive inhibitors with IC_{50} values of 8 μM and 10 μM, respectively (Tables 3 and 4; Figs. S14 and S15).

No IC_{50} values were calculated for the quaternary ammonium salts because they did not show notable inhibition of DAPI uptake (above the arbitrary threshold) at the selected concentration of 50 µM and under the experimental conditions used in the initial screening.

Table 3. Interaction strength analysis with DAPI as zebrafish Mate3 model substrate and set of selected compounds as interactors. Kinetic parameters of DAPI uptake are reported as apparent K_m ($_{Km,app}$) and apparent V_m ($V_{m,app}$) with 95% CI (confidence intervals). Data from a representative of at least three independent experiments are shown, each done in duplicate. For the IC_{50} calculations, data from at least three independent experiments were fitted to the sigmoidal four parameters dose-response model (variable slope) in GraphPad Prism 8. Experiments were done at pH 7.4. Substances that showed strong interaction are indicated in bold letters.

compound	IC_{50} [µM], N=3	95% CI	Interaction strength
n-butyltin	79.4	62.4 - 101	M
triethyltin	52.6	46.7 - 59.3	M
tri-n-propyltin	9.77	8.46 - 11.3	**St**
tri-n-butyltin	7.48	5.76 - 9.71	**St**
BDDAC	39.5	28.6 - 54.7	M
BDDA	5.25	3.98 - 6.93	**St**
BDHDA	49.5	32.3 - 75.9	M
quinidine	30.6	22.3 - 42.0	M
diltiazem	40.5	31.1 - 52.8	M
verapamil	5.29	4.19 - 6.68	**St**
acebutolol	25.2	19.5 - 32.7	**St**
mitoxantrone	1.24	0.98 - 1.56	**St**
doxorubicine	16.6	12.0 - 22.9	**St**
pyrimethamine	1.39	1.08 - 1.78	**St**
obidoxime	95.4	73.7 - 124	M
cimetidine	8.76	5.93 - 12.9	**St**
ranitidine	65.4	49.4 - 86.7	M

M – moderate strength; **St – strong interaction**; IC_{50} of < 1 µM - very strong (VSt) interactors; IC_{50} of 1–29 µM - strong (St) interactors; IC_{50} of 30–99 µM - moderate (M) interactors; IC_{50} of 100–999 µM - weak (W) interactors; IC_{50} > 1000 Mm - very weak (VW) interactors.

All tested cationic surfactants except DMDDDA showed notable interaction with zebrafish Mate3 protein, and their IC_{50} values were further determined. BDMDDA showed strong non-competitive inhibition with IC_{50} value of 5 μM, whereas BDMDA and BDMHDA showed moderate competitive inhibition with IC_{50} values of 40 and 50 μM, respectively (Tables 3 and 4; Figs. S14 and S15). To confirm that Mate3 in zebrafish is a predominantly cationic transporter, we also tested a wide range of nonionic surfactants and an anionic surfactant. As expected, none of the selected anionic and non-ionic surfactants showed interaction with zebrafish Mate3 protein at a concentration of 50 μM (Fig. 3).

Paraquat (PQT) showed no interaction at the selected concentration of 50 μM and under the selected experimental conditions (Fig. 3).

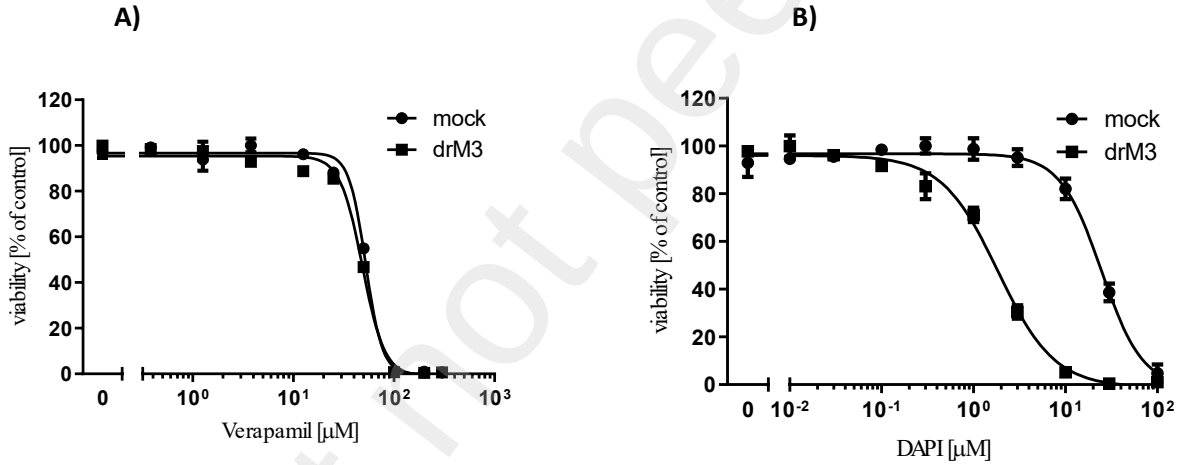

Figure 4. Cytotoxicity experiment aimed at determination of the type of interaction between the tested compounds and zebrafish Mate3. Example of an inhibitor (verapamil; **A**) and a substrate (DAPI; **B**) are shown. The MTT assay is used to measure cell viability, with the assumption that stable Mate3-transfected cells are more sensitive to the toxic effects of tested substrates compared to mock cells due to active transport by Mate3. EC_{50} values were calculated by fitting data from a representative experiment (done in duplicate) from at least three independent experiments to the sigmoidal four-parameter dose-response model (variable slope) using GraphPad Prism version 8.

3.6.2 Pharmaceuticals

Many of the 22 pharmaceuticals and personal care products tested showed significant interaction and were selected for additional characterization. The calcium channel blockers quinidine, diltiazem and verapamil showed moderate to strong interactions with IC_{50} values of 31, 41 and 5 µM, respectively (Table 3; Fig. S14). According to the toxicity modulation experiments, diltiazem and verapamil are non-competitive inhibitors (Table 4; Fig. S15). Acetobutolol, another antiarrhythmic drug and beta-blocker, showed a strong interaction with an IC_{50} value of 25 µM (Table 3) but was not used in toxicological experiments because of its low toxicity, so the type of the interaction was not determined (Table 4). The antineoplastic drugs mitoxantrone and doxorubicin showed a strong interaction with IC_{50} values of 1 and 17 µM, respectively, and they both acted as competitive inhibitors. Cimetidine, an H2 blocker and antiulcer drug, showed a strong interaction with zebrafish Mate3 with an IC_{50} value of 9 µM, and another H2 blocker, ranitidine, showed a moderate interaction with a corresponding IC_{50} value of 65. Unfortunately, the type of the interaction could not be determined for both H2 blockers because of their low toxicity in MTT assay (Tables 3 and 4; Fig. S14). The antimalarial drug pyrimethamine proved to be a strong interactor with an IC_{50} value of 1 µM but showed no toxicity, as did the oxime obidoxime, which showed a moderate interaction with an IC_{50} value of 95 µM (Tables 3 and 4; Fig. S14).

4. Discussion

Mate family of protein extruders plays an important role in the metabolism of endo- and xenobiotics in mammals. Nevertheless, comparatively little is known about the role of Mates in non-mammalian species, including zebrafish as an important model organism in biomedical and environmental research. Therefore, in this study we investigated the interaction of a wide range of environmentally and biomedically relevant compounds for their interaction with zebrafish Mate3.

To determine whether a compound interacts with zebrafish Mate3 transporter, at what strength, and by what type of inhibitory reaction, several sequential steps had to be applied in our study design. The main prerequisite was the development of a reliable transport activity assay, which in our study was based on the development of the HEK293 Flp-In cell line stably overexpressing Mate3 and the identification of suitable model fluorescent substrate(s). The assay needed to be

438 further optimized to achieve at least a semi-high throughput screening capacity. In addition, the
439 zebrafish Mate3 needed to be characterized in terms of the number of active sites, and the model
440 further tested and confirmed by potential docking of model substrates. Then, the developed assay
441 could have been used for initial screening studies of selected environmentally relevant compounds
442 and for determining the strength of their interaction.

443

444 **Table 4. Type of interaction between zebrafish Mate3 and interactors as determined by**
445 **modulating the cytotoxicity of the Mate3 interactors.** Sensitivity factors were calculated based
446 on the presumption that stably transfected Mate3 cells are more sensitive to the tested
447 substratesthan mock cells (MTT assay), due to the active transport of the respective substrates by
448 zebrafish Mate3 transporter. For EC_{50} calculations, data from at least three independent
449 experiments were fitted to the sigmoidal four parameter dose-response model (variable slope) in
450 GraphPad Prism version 8, using the data from the representative experiment (done in duplicate).

	mock		drM3			
compound	EC_{50} [µM]	95% CI	EC_{50} [µM]	95% CI	SF	TOI
mitoxantrone	3.81	0.96 - 15.1	0.21	0.19 - 0,25	18.1	S
acebutolol	not tox		not tox			ND
ranitidine	not tox		not tox			ND
verapamil	52.3	49.1 - 55.6	48.5	44.0 - 53.4	1.1	I
quinidine	nd		nd			
diltiazem	107	86.6 - 133	93.1	86.1 - 101	1.1	I
n-butyltin	not tox		not tox			ND
triethyltin	ND		ND			
TPrT	0.41	0.34 - 0.50	0.43	0.33 - 0.57	1.0	I
TBT	1.72	1.28 - 2.31	2.45	1.76 - 3.41	0.7	I
doxorubicine	0.16	0.12 - 0.21	0.01	0.006 - 0.016	16.0	S
pyrimethamine	not tox		not tox			ND
BDDAC	17.0	14.6 - 19.8	8.93	5.49 - 14.5	1.9	S
BDDA	9.69	8.35 - 11.2	9.42	7.65 - 11.6	1.0	I
BDHDA	16.7	14.9 - 18.7	4.68	3.86 - 5.66	3.6	S
obidoxime	not tox		not tox			ND
cimetidine	not tox		not tox			ND

not tox – compound not toxic in the solubility range applied; ND – not determined due to low toxicity; CI – confidence interval; SF – sensitivity factor, calculated as a ratio of EC_{50} values for mock versus EC_{50} values for Mate3 transfected cells; TOI – type of interaction

DAPI and ASP^+ were chosen as fluorescent model substrates because they allow us to measure uptake kinetics in real time, as they emit a fluorescent signal when they enter the cell through interaction with double-stranded DNA and intracellular proteins, respectively. Furthermore, since we wanted to observe whether different compounds are transported through the same active site, or whether Mate3 has a complex binding site, we used DAPI and ASP^+ to indirectly determine the number of binding sites by using one fluorescent compound as substrate and the second as an interactor and *vice versa*. The results showed that the zebrafish Mate3 transporter has a more complex binding region than expected (Fig. S5, Table 2), and our intention was to verify these experimental observations by homology modelling and molecular docking calculations using the 3D structure of zebrafish Mate3 predicted by the AlphaFold2 algorithm. In addition, because our previous work on the zebrafish Mate7 transporter showed that it probably has only one binding site for transport of its substrates (Lončar and Smital, 2018), the reliability of the obtained Mate3 model was additionally verified by comparing the Mate3 structure with the 3D structure of the zebrafish Mate7 transporter predicted in this study using the same algorithm.

In silico modelling is not a full substitute for crystal structures, so the credibility of the predicted Mate3 and Mate7 3D structures for transporter function analysis may be questionable. However, AlphaFold2 predicted high confidence values for amino acid coordinates in structurally and functionally important regions of both proteins. We performed parallel modelling, bioinformatic analysis, prediction of positions of TM segments and the topology (Tables S3-S5), and molecular docking on the Mate7 protein to verify the accuracy of the predicted 3D structures. The Mate3 and Mate7 proteins are sufficiently different with 44.7% sequence identity (Fig. S11A). Both proteins have 13 TM segments and an N-terminus located in the cytoplasmic space (Fig. S8), which is consistent with previous findings in the literature. The 13th TM segment evolved last and is probably not crucial for the function of Mate3 (Kusakizako et al., 2020).

The predicted 3D structure of zebrafish Mate3 was able to reproduce the mutual arrangement and connection of its 13 TM segments, which was independently confirmed by calculating the free

association energies and folding order of the TM segments using the TMPfold method (Lomize et al., 2020), i.e., the order of association of the TM segments (from the first - most energetically favourable): 3-4-2-5-6-1-7-8-9-10-11-12-13 (Table S5A). The most likely association pathway for the TM segments was determined (Table S5B), and the total ΔGassoc calculated by the TMPfold method was -134.1 kcal/mol, with the 13th TM segment having the smallest ΔGassoc, i.e. -6.4 kcal/mol (Fig. S10). These results are also consistent with previous literature reports (Kusakizako et al., 2020).

Finally, starting from the 3D structure of Mate3 and Mate7 proteins predicted by AlphaFold2, we performed molecular docking with the two model fluorescent substrates DAPI and ASP^+, for which the efficiency of passage across the membrane was measured in detail. We observed more negative energies (i.e. higher affinities) for both substrates in the centre than on the outer membrane part of the cavity. A higher gradient was observed for DAPI, which is in good agreement with experimental results (a lower K_m value was observed for DAPI than for ASP^+; Table 1). Molecular docking of DAPI and ASP^+ to Mate3 and Mate7 showed that the highest predicted affinity for DAPI and ASP^+ is associated with the conserved part of residues "EWW" on the 7th TM segment, which is co-conserved in Mate proteins of all higher organisms, including humans (Fig. S11B).

Consequently, as both our initial transport activity experiments and docking calculations performed with zebrafish Mate3 homology models showed a difference in the binding interactions between these two compounds, which could affect their transport differences, we could not proceed with performing Michaelis-Menten kinetics experiments to determine the nature of the interaction between the compounds and the transport protein. Therefore, we decided to perform modulation of toxicity experiments to obtain information about the compounds tested and the nature of their interaction with the zebrafish Mate3 transporter.

Furthermore, to understand the potential defensive role of zebrafish Mate3, it is also important to consider that the substrate specificity of MATEs is similar to that of organic cation transporters (OCTs), as these proteins cooperate in the renal elimination of endogenous compounds as well as xenobiotics (Chu et al., 2016; Hillgren et al., 2013; Morrissey et al., 2013; Motohashi & Inui, 2013a, 2013b; Nies et al., 2016; Otsuka et al., 2005). It can be surmised that there probably is a OCT-MATE vector transport by which different compounds are excluded, and that disruption of

511 the balance between these two proteins can lead to accumulation of toxins in the proximal tubules
512 (George et al., 2017; Staud et al., 2013). Zebrafish Oct1 may have a similar defensive role as the
513 human orthologs OCT1 and OCT2 (Mihaljević et al., 2017), which share overlapping substrate
514 specificities and occasionally similar substrate affinities (Nies et al., 2011). Accordingly, we
515 compared the results obtained for zebrafish Mate3 protein with both those reported for zebrafish
516 Oct1, due to their common cationic nature (Mihaljević et al., 2017), and those obtained for other
517 mammalian Mates. All previously reported data for mammalian Mates and for zebrafish Mate7
518 and Oct1 are presented in Tables S9 and S10 for comparison.

519 Based on these insights, we tested more than 30 industrial compounds (quaternary ammonium
520 salts, organotin compounds, and cationic surfactants) and identified several potent zebrafish Mate3
521 interactors (Fig. 3) that were selected for further analysis and determination of their IC_{50} values
522 (Table 3, Fig. S14). Among these compounds, organotin compounds (OTCs) are a cause of serious
523 environmental concern due to their highly toxic effects and bioaccumulation at low environmental
524 concentrations. Attention has been directed especially to tributyltin because of its highly toxic
525 effects and high bioaccumulation even at very low environmental concentrations (Borges et al.,
526 2014). Mihaljević et al. (2017) found that organotin compounds are the most potent xenobiotic
527 interactors of the zebrafish Oct1 transporter, with most potent effect determined for dibutyltin
528 chloride (DBT), followed by tributyltin (TBT) and tripropyltin chloride (TPrT) with IC_{50} values
529 in the low µM range. Lončar & Smital (2018) observed similar interaction potency of TPrT for
530 Mate7, while TBT was less potent and no interaction was observed for DBT up to 100 µM. In this
531 study, similar interaction pattern was observed for TPrT, with an IC_{50} value of 10 µM, which is in
532 the range previously shown for Oct1 and Mate7 (3 and 11 µM, respectively), and for TBT with an
533 IC_{50} value of 8 µM which is lower than for Mate7 (IC_{50} = 71 µM) and similar as for Oct1 (IC_{50} =
534 4 µM, (Mihaljević et al., 2017). N-butyltin trichloride (n-BT) and triethyltin (TET) appeared to be
535 less potent interactors with corresponding IC_{50} values of 80 µM and 53 µM, respectively. In
536 addition, interaction of n-BT with a zebrafish Mate protein was reported for the first time in this
537 study. Finally, our toxicological experiments (Table 4) showed that organotins are inhibitors of
538 Mate3 protein with similar affinities as for Oct1 (Mihaljević et al., 2017). These findings provide
539 important insights into the potential environmental impact of organotin compounds and highlight
540 the importance of further investigation into their interaction with Mate3 and other transporters.

None of the tested n-tetraalkylammonium compounds, known cationic model substances and a subgroup of quaternary ammonium compounds (QACs), showed any interaction with zebrafish Mate3. These data are in good agreement with results obtained by Lončar and Smital (2018), where TEA, which is considered as model MATE(s) cationic substrate, showed no interaction with zebrafish Mate7 in the range of 100 μM due to its IC_{50} value above 3 mM. Interestingly, we discovered that two cationic surfactants, BDDAC and BDHDA, showed moderate competitive inhibition (IC_{50} = 40 μM and 50 μM, respectively), while BDDA showed strong non-competitive inhibition of Mate3 transport (IC_{50} = 5 μM). To our knowledge, these are the first reported interactions between surfactants and any mammalian or fish MATEs/Mates.

Out of 22 pharmaceuticals and personal care products tested, 10 were identified as interactors. Obidoxime chloride, an antidote for organophosphate nerve poisoning, showed a moderate interaction with zebrafish Mate3 (IC_{50} = 95 μM), with no previously reported interactions with other MATE/ Mate proteins. A strong interaction with zebrafish Oct1 (IC_{50} = 0.4 μM) and strong inhibition with both human MATE proteins were observed for antimalarial drug pyrimethamine (Ito et al., 2010; Kusuhara et al., 2011). In our case, pyrimethamine showed strong interaction with zebrafish Mate3 (IC_{50} = 1 μM), similar to its strong competitive inhibition of zebrafish Mate7 (IC_{50} = 15 μM) reported previously (Lončar and Smital, 2018). Cimetidine exhibited high affinity as a substrate for both human MATEs, with low Michaelis constants of 8.0 μM and 18.2 μM, respectively. These were much lower than those for TEA (366 μM and 375 μM for hMATE1 and hMATE2-K, respectively; Ohta et al., 2009). In zebrafish, cimetidine showed a strong interaction with Mate3 (IC_{50} = 9 μM), but only a very weak interaction with Oct1 (IC_{50} = 522 μM). Acebutolol, a cardio-selective beta-blocker, showed weak competitive inhibition with zebrafish Mate7 (IC50 = 134 μM) in a previous study (Lončar and Smital, 2018), with no interactions reported with Oct1 and mammalian Mates. In this study, acebutolol showed a strong interaction with zebrafish Mate3 (IC50 = 9 μM), the first reported strong interaction of acetobutolol with any of the MATEs/Mates. Mitoxantrone, an antineoplastic antibiotic, showed in previously published studies a moderate interaction with zebrafish Oct1 (IC_{50} = 85 μM; Mihaljević at al., 2017), with strong non-competitive inhibition with Mate7 (IC_{50} = 4 μM, Lončar and Smital, 2018). In this study, mitoxantrone showed strong competitive inhibition (IC_{50} = 1 μM). Doxorubicin, an antineoplastic drug in the anthracycline class, was reported to show strong competitive inhibition of zebrafish Mate7 (IC_{50} = 14 μM, Lončar and Smital, 2018), and in this

study similar results were obtained for Mate3, where doxorubicin also showed strong competitive inhibition (IC_{50} = 17 μM). Verapamil, a Ca^{2+} blocker, that modifies calcium uptake by binding or exchanging calcium concentrations and affecting calcium levels that activate ATP-ase (Nayler and Szeto, 1972), interacts with both human MATEs and shows an inhibitory type of reaction (Tanihara et al., 2007). In several studies, verapamil showed a significant inhibitory effect on the efflux pump activity of mycobacteria (Adams et al., 2011; Machado et al., 2012). This study suggests that verapamil is strong inhibitor (IC_{50} = 5 μM) which is in good agreement with results obtained for Oct1 (IC_{50} = 14 μM, Mihaljević et al., 2017) and for zebrafish Mate7 (IC_{50} = 3 μM, (Lončar and Smital, 2018). Diltiazem, an antihypertensive and vasodilator agent that acts by relaxing vascular muscles to lower blood pressure, showed moderate interaction with zebrafish Oct1 (IC_{50} = 62 μM; Mihaljević et al., 2017) and moderate non-competitive inhibition of Mate 7 (IC_{50} = 51 μM, Lončar and Smital, 2018). This study showed similar results for Mate3 (IC_{50} = 41 μM, moderate non-competitive inhibitor).

Finally, in addition to the indication of the type of the interaction, modulation of toxicity experiments performed in this study (Table 4, Fig. 4) showed that Mate3 stably transfected cells are, as expected, more sensitive to toxic effects of fluorescent substrates than mock cells due to the Mate3 active transport of substrates. However, analysis of EC_{50} and IC_{50} values revealed that some compounds exhibited toxic effects at concentrations lower than their interaction strength (IC50 values) (Tables 3 and 4). These compounds, such as tripropyltin chloride, tributyltin, doxorubicin, BDDAC, and BDHDA, are moderate to strong interactors with potent toxicity, indicating that compounds with high affinity for the protein of interest can have strong physiological effects even at low concentrations. While the industrial compounds that interacted with zebrafish Mate3 in this study are likely to be of low ecotoxicological relevance based on reported environmental concentrations, bioaccumulation processes may be important when aquatic organisms are chronically exposed to high concentrations of contaminants. In these cases, the observed affinities in the low micromolar range may be strong enough to modulate and disrupt the protective efflux activity of Mate3.

5. Conclusions

In this study we developed and optimized a highly specific screening assay and performed the first characterization of zebrafish Mate3 xenobiotic interactors. By combining the assay with the

zebrafish Mate3 homology model, we identified potent Mate3 inhibitors among various classes of environmental contaminants. Some of the identified interactors may be of environmental concern as they could disrupt the normal efflux function of Mate3, making fish more sensitive to harmful substances that commonly enter the aquatic environment. Our findings also highlight the importance of considering the differences in substrate preferences of Mate3 in zebrafish compared to Mates in mammals when employing zebrafish as a model organism in pharmacological and toxicological research.

In addition, we believe that the demonstrated quality of the 3D structure of Mate3 and Mate7 proteins as predicted by the AlphaFold2 algorithm opens the possibility of successfully applying this tool for *in silico* predictions of the transport preferences of Mate3 and Mate7 proteins, and possibly other Mate transporters. It will be interesting to see in future research whether the 3D structures predicted by AlphFold2 will also be (and how, i.e., to what extent) sensitive and accurate for identifying point mutations that may critically modulate the transport activity of Mate proteins

CRediT authorship contribution statement

L. Vujica: conceptualization, interaction studies and toxicity experiments, writing – original draft. **J. Lončar**: development of stable transfectants, expression analysis, writing – review & editing. **L. Mišić**: assay development for interaction studies, toxicity experiments. **B. Lučić**: homology modelling and model analysis, writing – review & editing. **K. Radman**: molecular docking studies. **I. Mihaljević**: conceptualization, *in silico* interaction studies, writing – review & editing. **B. Bertoša**: supervision of molecular docking studies, writing – review & editing; **J. Mesarić**: preparation and input of data for homology modelling; **M. Horvat**: interaction studies. **T. Smital**: conceptualization, writing – review & editing, supervision, project administration, funding acquisition.

Declaration of competing interest

The authors declare that they have no known competing financial interests or personal relationships that could have appeared to influence the work reported in this paper.

Acknowledgements

This work was supported by the Croatian Science Foundation (Project No. IP-2019–04-1147 granted to T. Smital), and by the STIM-REI Centre for Excellence project, Contract Number: KK.01.1.1.01.0003 funded by the European Union through the European Regional Development Fund – Operational Programme Competitiveness and Cohesion 2014–2020 (KK.01.1.1.01). All computer simulations in this study were performed on the Bura supercomputer, which was procured under the project "Development of research infrastructure at the University campus in Rijeka", co-funded by the European Regional Development Fund (ERDF).

Appendix A. Supplementary data

Supplementary material related to this article can be found, in the online version, at doi:

References

1. Adams, K. N., Takaki, K., Connolly, L. E., Wiedenhoft, H., Winglee, K., Humbert, O., Edelstein, P. H., Cosma, C. L., & Ramakrishnan, L. (2011). Drug Tolerance in Replicating Mycobacteria Mediated by a Macrophage-Induced Efflux Mechanism. *Cell*, *145*(1), 39–53. https://doi.org/10.1016/j.cell.2011.02.022
2. Bernsel, A., Viklund, H., Hennerdal, A., & Elofsson, A. (2009). TOPCONS: Consensus prediction of membrane protein topology. *Nucleic Acids Research*, *37*(Web Server), W465–W468. https://doi.org/10.1093/nar/gkp363
3. Borges, A. R., López-Serrano Oliver, A., Gallego-Gallegos, M., Muñoz-Olivas, R., Rodrigues Vale, M. G., & Cámara, C. (2014). Transformation of tributyltin in zebrafish eleutheroembryos (Danio rerio). *Biological Trace Element Research*, *162*(1–3), 317–323. https://doi.org/10.1007/s12011-014-0144-z
4. Bradford, M. M. (1976). A rapid and sensitive method for the quantitation of microgram quantities of protein utilizing the principle of protein-dye binding. *Analytical Biochemistry*, *72*(1), 248–254. https://doi.org/10.1016/0003-2697(76)90527-3

5. Chu, X., Bleasby, K., Chan, G. H., Nunes, I., & Evers, R. (2016). The Complexities of Interpreting Reversible Elevated Serum Creatinine Levels in Drug Development: Does a Correlation with Inhibition of Renal Transporters Exist? *Drug Metabolism and Disposition*, *44*(9), 1498–1509. https://doi.org/10.1124/dmd.115.067694
6. Clerbaux, L.-A., Coecke, S., Lumen, A., Kliment, T., Worth, A. P., & Paini, A. (2018). Capturing the applicability of in vitro-in silico membrane transporter data in chemical risk assessment and biomedical research. *Science of The Total Environment*, *645*, 97–108. https://doi.org/10.1016/j.scitotenv.2018.07.122
7. Damme, K., Nies, A. T., Schaeffeler, E., & Schwab, M. (2011). Mammalian MATE (SLC47A) transport proteins: Impact on efflux of endogenous substrates and xenobiotics. *Drug Metabolism Reviews*, *43*(4), 499–523. https://doi.org/10.3109/03602532.2011.602687
8. Dobson, L., Szekeres, L. I., Gerdán, C., Langó, T., Zeke, A., & Tusnády, G. E. (2023). TmAlphaFold database: Membrane localization and evaluation of AlphaFold2 predicted alpha-helical transmembrane protein structures. *Nucleic Acids Research*, *51*(D1), D517–D522. https://doi.org/10.1093/nar/gkac928
9. George, B., You, D., Joy, M. S., & Aleksunes, L. M. (2017). Xenobiotic transporters and kidney injury. *Advanced Drug Delivery Reviews*, *116*, 73–91. https://doi.org/10.1016/j.addr.2017.01.005
10. Hiasa, M., Matsumoto, T., Komatsu, T., & Moriyama, Y. (2006). Wide variety of locations for rodent MATE1, a transporter protein that mediates the final excretion step for toxic organic cations. *American Journal of Physiology-Cell Physiology*, *291*(4), C678–C686. https://doi.org/10.1152/ajpcell.00090.2006
11. Hiasa, M., Matsumoto, T., Komatsu, T., Omote, H., & Moriyama, Y. (2007). Functional characterization of testis-specific rodent multidrug and toxic compound extrusion 2, a class III MATE-type polyspecific H+/organic cation exporter. *American Journal of Physiology. Cell Physiology*, *293*, C1437-44. https://doi.org/10.1152/ajpcell.00280.2007
12. Hillgren, K. M., Keppler, D., Zur, A. A., Giacomini, K. M., Stieger, B., Cass, C. E., Zhang, L., & International Transporter Consortium. (2013). Emerging transporters of clinical importance: An update from the International Transporter Consortium. *Clinical Pharmacology and Therapeutics*, *94*(1), 52–63. https://doi.org/10.1038/clpt.2013.74

13. Humphrey, W., Dalke, A., & Schulten, K. (1996). VMD: Visual molecular dynamics. *Journal of Molecular Graphics*, *14*(1), 33–38. https://doi.org/10.1016/0263-7855(96)00018-5
14. Ito, S., Kusuhara, H., Kuroiwa, Y., Wu, C., Moriyama, Y., Inoue, K., Kondo, T., Yuasa, H., Nakayama, H., Horita, S., & Sugiyama, Y. (2010). Potent and specific inhibition of mMate1-mediated efflux of type I organic cations in the liver and kidney by pyrimethamine. *Journal of Pharmacology and Experimental Therapeutics*, *333*(1), 341–350. https://doi.org/10.1124/jpet.109.163642
15. Jumper, J., Evans, R., Pritzel, A., Green, T., Figurnov, M., Ronneberger, O., Tunyasuvunakool, K., Bates, R., Žídek, A., Potapenko, A., Bridgland, A., Meyer, C., Kohl, S. A. A., Ballard, A. J., Cowie, A., Romera-Paredes, B., Nikolov, S., Jain, R., Adler, J., … Hassabis, D. (2021). Highly accurate protein structure prediction with AlphaFold. *Nature*, *596*(7873), 583–589. https://doi.org/10.1038/s41586-021-03819-2
16. Kapuscinski, J. (1995). DAPI: A DNA-Specific Fluorescent Probe. *Biotechnic & Histochemistry*, *70*(5), 220–233. https://doi.org/10.3109/10520299509108199
17. Kobara, A., Hiasa, M., Matsumoto, T., Otsuka, M., Omote, H., & Moriyama, Y. (2008). A novel variant of mouse MATE-1 H+/organic cation antiporter with a long hydrophobic tail. *Archives of Biochemistry and Biophysics*, *469*(2), 195–199. https://doi.org/10.1016/j.abb.2007.10.010
18. Kusakizako, T., Miyauchi, H., Ishitani, R., & Nureki, O. (2020). Structural biology of the multidrug and toxic compound extrusion superfamily transporters. *Biochimica et Biophysica Acta (BBA) - Biomembranes*, *1862*(12), 183154. https://doi.org/10.1016/j.bbamem.2019.183154
19. Kusuhara, H., Ito, S., Kumagai, Y., Jiang, M., Shiroshita, T., Moriyama, Y., Inoue, K., Yuasa, H., & Sugiyama, Y. (2011). Effects of a MATE protein inhibitor, pyrimethamine, on the renal elimination of metformin at oral microdose and at therapeutic dose in healthy subjects. *Clinical Pharmacology and Therapeutics*, *89*(6), 837–844. https://doi.org/10.1038/clpt.2011.36
20. Lomize, A. L., Pogozheva, I. D., & Mosberg, H. I. (2011). Anisotropic Solvent Model of the Lipid Bilayer. 2. Energetics of Insertion of Small Molecules, Peptides, and Proteins in

Membranes. *Journal of Chemical Information and Modeling*, *51*(4), 930–946. https://doi.org/10.1021/ci200020k

21. Lomize, A. L., Schnitzer, K. A., & Pogozheva, I. D. (2020). TMPfold: A Web Tool for Predicting Stability of Transmembrane α-Helix Association. *Journal of Molecular Biology*, *432*(11), 3388–3394. https://doi.org/10.1016/j.jmb.2019.10.024
22. Lomize, A. L., Todd, S. C., & Pogozheva, I. D. (2022). Spatial arrangement of proteins in planar and curved membranes by PPM 3.0. *Protein Science*, *31*(1), 209–220. https://doi.org/10.1002/pro.4219
23. Lomize, M. A., Pogozheva, I. D., Joo, H., Mosberg, H. I., & Lomize, A. L. (2012). OPM database and PPM web server: Resources for positioning of proteins in membranes. *Nucleic Acids Research*, *40*(Database issue), D370-376. https://doi.org/10.1093/nar/gkr703
24. Lončar, J., Popović, M., Krznar, P., Zaja, R., & Smital, T. (2016). The first characterization of multidrug and toxin extrusion (MATE/SLC47) proteins in zebrafish (Danio rerio). *Scientific Reports*, *6*(1), 28937. https://doi.org/10.1038/srep28937
25. Lončar, J., & Smital, T. (2018). Interaction of environmental contaminants with zebrafish (Danio rerio) multidrug and toxin extrusion protein 7 (Mate7/Slc47a7). *Aquatic Toxicology (Amsterdam, Netherlands)*, *205*, 193–203. https://doi.org/10.1016/j.aquatox.2018.10.016
26. Luckenbach, T., Fischer, S., & Sturm, A. (2014). Current advances on ABC drug transporters in fish. *Comparative Biochemistry and Physiology Part C: Toxicology & Pharmacology*, *165*, 28–52. https://doi.org/10.1016/j.cbpc.2014.05.002
27. Machado, D., Couto, I. M. dos S. L., Perdigão, J., Rodrigues, L., Portugal, I., Baptista, P., Veigas, B., Amaral, L., & Bettencourt, M. V. (2012). Contribution of Efflux to the Emergence of Isoniazid and Multidrug Resistance in Mycobacterium tuberculosis. *PLoS ONE*, *7*(4). https://doi.org/10.1371/journal.pone.0034538
28. Mariani, V., Biasini, M., Barbato, A., & Schwede, T. (2013). lDDT: A local superposition-free score for comparing protein structures and models using distance difference tests. *Bioinformatics*, *29*(21), 2722–2728. https://doi.org/10.1093/bioinformatics/btt473
29. Masuda, S., Terada, T., Yonezawa, A., Tanihara, Y., Kishimoto, K., Katsura, T., Ogawa, O., & Inui, K. (2006). Identification and functional characterization of a new human kidney-specific H+/organic cation antiporter, kidney-specific multidrug and toxin

extrusion 2. *Journal of the American Society of Nephrology*, *17*(8), 2127–2135. https://doi.org/10.1681/asn.2006030205

30. Mihaljević, I., Popović, M., Žaja, R., Maraković, N., Šinko, G., & Smital, T. (2017). Interaction between the zebrafish (Danio rerio) organic cation transporter 1 (Oct1) and endo- and xenobiotics. *Aquatic Toxicology (Amsterdam, Netherlands)*, *187*, 18–28. https://doi.org/10.1016/j.aquatox.2017.03.012
31. Morris, G. M., Huey, R., Lindstrom, W., Sanner, M. F., Belew, R. K., Goodsell, D. S., & Olson, A. J. (2009). AutoDock4 and AutoDockTools4: Automated docking with selective receptor flexibility. *Journal of Computational Chemistry*, *30*(16), 2785–2791. https://doi.org/10.1002/jcc.21256
32. Morrissey, K. M., Stocker, S. L., Wittwer, M. B., Xu, L., & Giacomini, K. M. (2013). Renal transporters in drug development. *Annual Review of Pharmacology and Toxicology*, *53*, 503–529. https://doi.org/10.1146/annurev-pharmtox-011112-140317
33. Mosmann, T. (1983). Rapid colorimetric assay for cellular growth and survival: Application to proliferation and cytotoxicity assays. *Journal of Immunological Methods*, *65*(1–2), 55–63. https://doi.org/10.1016/0022-1759(83)90303-4
34. Motohashi, H., & Inui, K. (2013a). Multidrug and toxin extrusion family SLC47: Physiological, pharmacokinetic and toxicokinetic importance of MATE1 and MATE2-K. *Molecular Aspects of Medicine*, *34*(2–3), 661–668. https://doi.org/10.1016/j.mam.2012.11.004
35. Motohashi, H., & Inui, K. (2013b). Organic cation transporter OCTs (SLC22) and MATEs (SLC47) in the human kidney. *The AAPS Journal*, *15*(2), 581–588. https://doi.org/10.1208/s12248-013-9465-7
36. Nayler, W. G., & Szeto, J. (1972). Effect of verapamil on contractility, oxygen utilization, and calcium exchangeability in mammalian heart muscle. *Cardiovascular Research*, *6*(2), 120–128. https://doi.org/10.1093/cvr/6.2.120
37. Nies, A. T., Damme, K., Kruck, S., Schaeffeler, E., & Schwab, M. (2016). Structure and function of multidrug and toxin extrusion proteins (MATEs) and their relevance to drug therapy and personalized medicine. *Archives of Toxicology*, *90*(7), 1555–1584. https://doi.org/10.1007/s00204-016-1728-5

38. Nies, A. T., Hofmann, U., Resch, C., Schaeffeler, E., Rius, M., & Schwab, M. (2011). Proton Pump Inhibitors Inhibit Metformin Uptake by Organic Cation Transporters (OCTs). *PLoS ONE*, *6*(7), e22163. https://doi.org/10.1371/journal.pone.0022163
39. Ohta, K., Inoue, K., Hayashi, Y., & Yuasa, H. (2006). Molecular Identification and Functional Characterization of Rat Multidrug and Toxin Extrusion Type Transporter 1 as an Organic Cation/H+ Antiporter in the Kidney. *Drug Metabolism and Disposition*, *34*(11), 1868–1874. https://doi.org/10.1124/dmd.106.010876
40. Ohta, K., Inoue, K., Yasujima, T., Ishimaru, M., & Yuasa, H. (2009). Functional Characteristics of Two Human MATE Transporters: Kinetics of Cimetidine Transport and Profiles of Iinhibition by Various Compounds. *Journal of Pharmacy & Pharmaceutical Sciences*, *12*(3), Article 3. https://doi.org/10.18433/J3R59X
41. Otsuka, M., Matsumoto, T., Morimoto, R., Arioka, S., Omote, H., & Moriyama, Y. (2005). A human transporter protein that mediates the final excretion step for toxic organic cations. *Proceedings of the National Academy of Sciences*, *102*(50), 17923–17928. https://doi.org/10.1073/pnas.0506483102
42. Schrödinger. (2021). Maestro. LLC.
43. Shin, N., Oh, J.-H., & Lee, Y.-J. (2015). Role of drug transporters: An overview based on knockout animal model studies. *Journal of Pharmaceutical Investigation*, *45*(2), 101–114. https://doi.org/10.1007/s40005-015-0178-z
44. Staud, F., Cerveny, L., Ahmadimoghaddam, D., & Ceckova, M. (2013). Multidrug and toxin extrusion proteins (MATE/SLC47); role in pharmacokinetics. *The International Journal of Biochemistry & Cell Biology*, *45*(9), 2007–2011. https://doi.org/10.1016/j.biocel.2013.06.022
45. Tanihara, Y., Masuda, S., Sato, T., Katsura, T., Ogawa, O., & Inui, K. (2007). Substrate specificity of MATE1 and MATE2-K, human multidrug and toxin extrusions/H+-organic cation antiporters. *Biochemical Pharmacology*, *74*(2), 359–371. https://doi.org/10.1016/j.bcp.2007.04.010
46. Trott, O., & Olson, A. J. (2009). AutoDock Vina: Improving the speed and accuracy of docking with a new scoring function, efficient optimization, and multithreading. *Journal of Computational Chemistry*, NA-NA. https://doi.org/10.1002/jcc.21334

47. Williams, C. J., Headd, J. J., Moriarty, N. W., Prisant, M. G., Videau, L. L., Deis, L. N., Verma, V., Keedy, D. A., Hintze, B. J., Chen, V. B., Jain, S., Lewis, S. M., Arendall, W. B., Snoeyink, J., Adams, P. D., Lovell, S. C., Richardson, J. S., & Richardson, D. C. (2018). MolProbity: More and better reference data for improved all-atom structure validation. *Protein Science: A Publication of the Protein Society*, *27*(1), 293–315. https://doi.org/10.1002/pro.3330

48. Xie, H. (2008). Activity assay of membrane transport proteins. *Acta Biochimica Et Biophysica Sinica*, *40*(4), 269–277. https://doi.org/10.1111/j.1745-7270.2008.00400.x

49. Zhang, X., Cherrington, N. J., & Wright, S. H. (2007). Molecular identification and functional characterization of rabbit MATE1 and MATE2-K. *American Journal of Physiology-Renal Physiology*, *293*(1), F360–F370. https://doi.org/10.1152/ajprenal.00102.2007

50. Zhang, X., He, X., Baker, J., Tama, F., Chang, G., & Wright, S. H. (2012). Twelve Transmembrane Helices Form the Functional Core of Mammalian MATE1 (Multidrug and Toxin Extruder 1) Protein. *Journal of Biological Chemistry*, *287*(33), 27971–27982. https://doi.org/10.1074/jbc.M112.386979

51. Zhang, X., & Wright, S. H. (2009). MATE1 has an external COOH terminus, consistent with a 13-helix topology. *American Journal of Physiology-Renal Physiology*, *297*(2), F263–F271. https://doi.org/10.1152/ajprenal.00123.2009